RESEARCH ARTICLE

Sokoto Journal of Veterinary Sciences

(P-ISSN 1595-093X: E-ISSN 2315-6201)

http://dx.doi.org/10.4314/sokjvs.v20i5.6

Peter-Ajuzie & Nwaogu /*Sokoto Journal of Veterinary Sciences*, **20**(Special): 54 – 62.

Morphological evaluation of the orbit and peri-ocular glands of the African grasscutter (*Thryonomys swinderianus*)

IK Peter-Ajuzie* & IC Nwaogu

Department of Veterinary Anatomy, Faculty of Veterinary Medicine, University of Nigeria, Nigeria

*Correspondence: Tel.: +2347030518464; E-mail: iheanyi.peter-ajuzie@unn.edu.ng

Publication History:
Received: 26-12-2021
Revised: 29-01-2022
Accepted: 14-02-2022

Abstract

The morphological features of the orbit and peri-ocular glands of the herbivorous African grasscutter were evaluated in this study. Heads of the rats were processed using the cold-water maceration technique, while the peri-ocular glands were obtained and processed for light microscopy using the conventional paraffin technique. The orbit was laterally located and associated with an enlarged maxillary infraorbital foramen. This orbital configuration imparted the grasscutter with a panoramic field of vision and a hystricomorphous improved masticatory ability. The Zeis and meibomian glands were located in the eyelid and showed holocrine histological features with myoepithelial cells surrounding their secretory acini. The gland of Moll was a simple coiled tubular gland that, together with the gland of Zeis, were associated with the palpebral cilia. The large harderian gland situated posterior to the eyeball was a lobulated compound exocrine gland whose secretory cells contained basally-displaced nuclei and foamy cytoplasm. The protruding glandular mass located adjacent to the rostral half of the upper eyelid, which we named the suprapalpebral gland had similar histological features as the harderian gland. These peri-ocular glands produced mainly mucoid and lipid secretions required for maintenance of structural and functional integrity of the cornea and eyelid. The qualitative and quantitative data from this study will be useful in the understanding of the biology of the African grasscutter and in the identification of orbital and peri-ocular glandular pathology in this species.

Keywords: Meibomian gland, Orbit, Peri-ocular glands, Suprapalpebral gland, *Thryonomys swinderianus*

Introduction

The African grasscutter, *Thryonomys swinderianus,* is a nocturnal herbivorous rodent that is aggressively hunted for its meat. It is a hystricognathous rodent that belongs to the family thryonomydae, believed to have originated from Africa (Sallam *et al.*, 2011). The rodent is fossorial and spends its day in dark burrows but moves about at night in search of food (Obadiah *et al.*, 2015; Igbokwe *et al.*, 2017). The grasscutter is also considered as an agricultural pest as it is known to feed on crops such as sugarcane, wheat, maize, and cassava (Igado *et al.*, 2016). The demand for its meat together with its ability to breed in confinement, has resulted in grasscutter farming in West Africa and the increasing search for knowledge of the peculiar biology of the species (Peter-Ajuzıe *et al.*, 2019).

The mammalian eye is the organ of sight comprising three tunics viz, the corneo-sclera, uvea and retina. The grasscutter has a rod-dominated retina (Lau &

Linsenmeier, 2012) and has been reported to have poor eyesight (Igbokwe *et al*., 2017). It is said to be visually adapted for inferior nocturnal vision as a result of high corneal diameter to eye diameter ratio, scanty retinal ganglion cells, and absence of tapetum lucidum (Peter-Ajuzıe *et al*., 2019). Knowledge of its orbital and associated ocular glands morphologies are however scant. This greatly hampers the understanding of its visual characteristics which would be useful in grasscutter farming and biomedical research. This study, therefore, investigated the morphology of the orbit and ocular glands of the African grasscutter and discussed the significance of the observed morphological characteristics.

Materials and Methods

Experimental animals

Ten male African grasscutters obtained from a grasscutter farm in Nike, Enugu East L.G.A. of Enugu State, Nigeria, were used for this study. They had a mean weight of 1.04 ± 0.56 kg and a mean age of 4.05 ± 1.44 months. After euthanasia using intramuscular injections of xylazine hydrochloride (7 mg/kg) and ketamine hydrochloride (120 mg/kg), samples of the eyelid, harderian gland and suprapalpebral protuberance were resected using scalpel blade and fixed in 10% neutral buffered formalin for histological examination. This suprapalpebral protuberance was a soft pointed protuberance situated on the facial skin adjacent to the rostral half of the upper eyelid. The head was thereafter decapitated at the atlanto-occipital joint, weighed, and prepared for orbital studies.

This study was approved by the Institutional Animal Care and Use Committee of the Faculty of Veterinary Medicine, University of Nigeria (approval number: FVM-UNN-IACUC-2019-1132).

Orbital studies

Preparation of skulls for orbital studies was carried out according to the cold water maceration technique (Sullivan & Romney, 1999). Each head of the animals was soaked in water at room temperature after the removal of adhering soft tissues. After two to three weeks of soaking, the remaining soft tissues were completely removed and the skulls were left to dry. The bones of the orbit were studied and identified as described in other related species (Miller, 2008; Samuelson, 2014). The Skull weight, orbital diameter, orbital depth, orbital axis angle, and orbital volume were measured. The skull weight was measured using a weighing balance. The orbital diameter was measured as the distance from orbital margin of lacrimal bone to orbital margin of zygomatico-temporal joint (Plate 1). The orbital depth was measured as the maximum distance from the orbital apex to the orbital margin of zygomatico-temporal joint (Plate 1). The orbital apex is the most medial point of the orbital wall located at the interforamina area between the caudal and cranial groups of orbital foramina. The orbital axis angle was measured as the angle between the orbital axis of the orbit and the median plane (Plate 1). The orbital axis is a line that

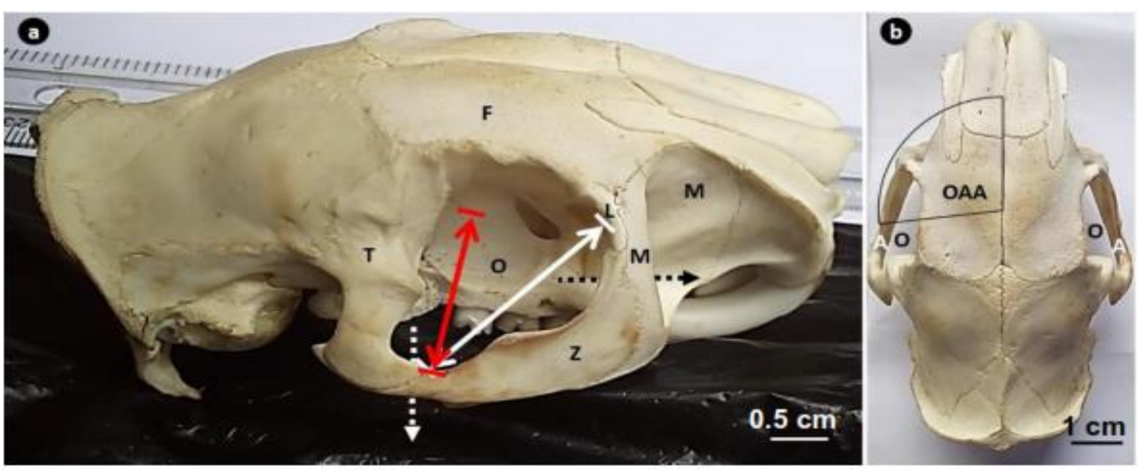

Plate 1: The orbit of the African grasscutter

Skull of the African grasscutter showing the orbit and its associated structures. **a.** The orbital opening proper (O) bounded by the frontal (F), temporal (T), lacrimal (L), and zygomatic (Z) bones. The maxilla (M) surrounds the enlarged infraorbital foramen (black dotted arrow passes through it). Ventro-caudal opening (white dotted arrow passes through it), orbital diameter (white solid arrow), and orbital depth (red solid arrow) are shown. **b.** The zygomatic arch (A), orbital opening (O), and orbital axes angle (OAA) are shown runs from the orbital apex to the center of the lateral orbital opening (Miller, 2008). The orbital volume was obtained using a modified procedure of the water filling method (Acer *et al.*, 2009). In this procedure, a water-proof polythene material was fitted into the orbit and a known volume of water was introduced into the material until the entire orbit was filled with water. The volume of water introduced was taken as the orbital volume.

Ocular gland histology

The samples of the eyelid, harderian gland, and suprapalpebral gland which were fixed in 10% neutral buffered formalin were dehydrated in increasing concentrations of ethanol, and subsequently processed routinely for light microscopy. 5 - 6 µm thick sections obtained were thereafter stained using haematoxylin and eosin staining protocol and Masson's trichrome staining protocol. Moticam Images Plus 2.0 digital camera (Motic China Group Ltd., China) was used to obtain photomicrographs of histological sections.

Data analysis

Data obtained from the study were presented as mean ± standard deviation.

Results

The orbit was located laterally within the skull with a complete bony orbital rim. The **s**kull and head weights were $1.60 \times 10^{-2} \pm 6.55 \times 10^{-3}$ kg and $1.12 \times 10^{-1} \pm 1.29 \times 10^{-2}$ kg respectively. The **s**kull weight was thus about 14% of head weight. Osteometric parameters of the orbit are shown in Table 1. The orbit was associated with three large openings situated at its rostral, lateral, and ventro-caudal aspects (Plate 1). The rostral opening was the enlarged infraorbital foramen of the maxillary bone, while the lateral opening was the orbital opening proper which was bounded by the frontal, lacrimal, zygomatic, and temporal bones. The ventro-caudal opening was extensive and occupied the ventral and caudal aspects of the orbit. It was bounded by the temporal, palatine, sphenoid, maxillary, and zygomatic bones. The zygomatic arch, formed by the zygomatic, temporal and maxillary bones, separated the orbital opening properly from the ventro-caudal opening. The lacrimal and maxillary bones formed the rostral wall of the orbital cavity while the frontal bone occupied its dorsal and medial boundaries (Plate 1). The caudal bony boundary was occupied by the temporal bone, while the lateral boundary was formed by the zygomatic arch. The ventral and medial walls were occupied by the sphenoid, palatine, and maxillary (alveolar part) bones.

The meibomian or tarsal glands were the most conspicuous and numerous of the three sets of glandular tissues observed in the eyelid. These glands were characterized by numerous round and elongated secretory acini aggregated in the tarsal plate with their secretory ducts (Plate 2). Each acinus lacked central luminal space and was surrounded by a basement membrane on which sat a basal layer of squamous myoepithelial cells. The interior of the acinus comprised polygonal mononuclear secretory cells at different levels of maturation with foamy, pale-staining cytoplasm and largely euchromatic, centrally-located nuclei (Plate 2). Evidence of nuclear disintegration, nuclear pyknosis and loss of cell outlines were observed in mature secretory cells. Cells resembling fibrocytes were seen dispersed in the interstitial loose connective tissue between the acini. The collecting ductules and central duct of the gland were lined by keratinized stratified squamous epithelium and contained remnants of the secretory cells. The keratinized epithelial lining of the collecting ductules thinned down significantly to become a tissue spur on entering the central duct. These collecting ductules characteristically opened obliquely into the central duct.

The sebaceous glands of Zeis were arranged in clusters of one to three acini closely associated with each hair follicle of the eyelid (Plate 3). They were less numerous than the meibomian gland in the eyelid. Both glands of Zeis and meibomian glands shared some secretory acinar morphological features such as lack of central luminal space, pale-staining cytoplasm, cellular mononuclearity, centrally-located nuclei, and presence of surrounding myoepithelial cells. The secretory cells of the gland of Zeis were, however, round in shape.

The glands of Moll were simple coiled tubular glands found within the tarsal plate. Their ducts opened into

Table 1: Osteometric parameters of the orbit of the African grasscutter

S/No	Parameter (n=10)	Mean	Standard deviation	Range
1	Orbital Volume (l)	2.02×10^{-3}	9.40×10^{-4}	1.40×10^{-3} - 4.05×10^{-3}
2	Orbital Diameter (m)	1.87×10^{-2}	1.60×10^{-3}	1.69×10^{-2} - 2.20×10^{-2}
3	Orbital Depth (m)	1.84×10^{-2}	1.50×10^{-3}	1.64×10^{-2} - 2.14×10^{-2}
4	Orbital Axis Angle (°)	101.15	6.71	83.50 - 113.00

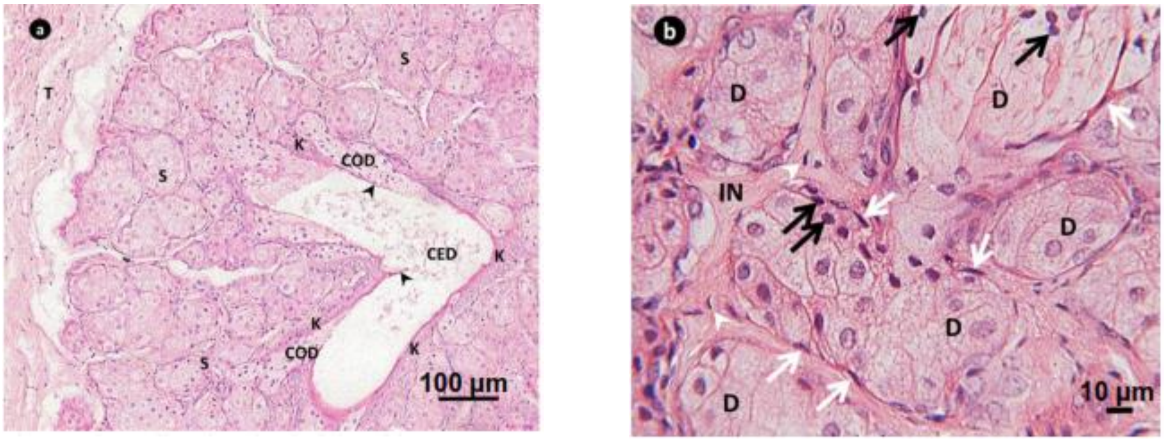

Plate 2: The meibomian gland of the African grasscutter
Meibomian gland of the African grasscutter showing its secretory acini and ducts. **a.** Central duct (CED) containing secretory materials and collecting ductule (COD) containing secretory cells are surrounded by secretory acini (S). The ducts are lined by keratinized stratified squamous epithelium (K). Tissue spurs (black arrowheads) and dense connective tissue of the tarsal plate (T) are shown. Haematoxylin and eosin stain. **b**. Higher magnification of secretory acini containing disintegrating nuclei and cell boundaries of mature cells (D) and surrounded by myoepithelial cells (white arrows). Pyknotic nuclei (black arrows), interstitial tissue (IN), and fibrocytes (white arrowheads) are shown. Haematoxylin and eosin stain

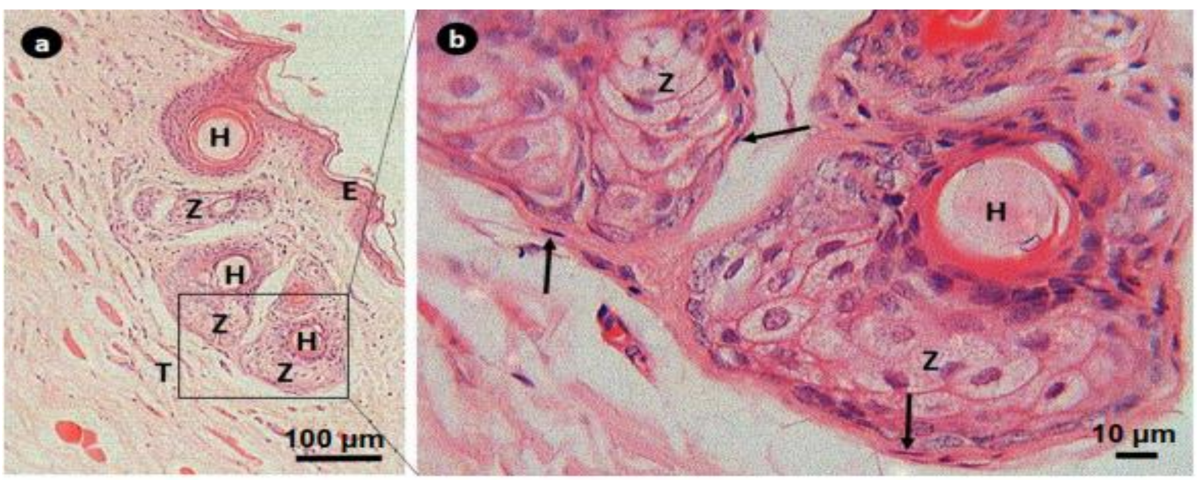

Plate 3: The gland of Zeis of the African grasscutter
a. Eyelid of the African grasscutter showing secretory cells of the glands of Zeis (Z) with associated hair follicles (H), keratinized stratified squamous epithelium of the epidermis (E), and dense irregular connective tissue of the tarsal plate (T). Haematoxylin and eosin stain. **b.** Enlarged view of glands of Zeis (Z) with associated hair follicles (H) and myoepithelial cells (arrows). Haematoxylin and eosin stain

the hair follicles of the eyelid (Plate 4). They were the scantiest and smallest of the glands of the eyelid. The secretory acinus and duct were lined by simple cuboidal epithelium and had lumen. The epithelial cells were mononucleated and had centrally-located nuclei and deeply acidophilic cytoplasm. Blood vessels were observed surrounding the gland.

The macroscopically visible harderian gland was a pink soft tissue mass situated posterior to the eyeball in the orbit. It was slightly larger than the eye and was triangular in outline (Plate 5). Histologically, it was a lobulated compound exocrine gland surrounded by a capsular layer of simple squamous epithelium. The secretory acini were simple columnar epithelia containing round basally displaced nuclei and apical foamy cytoplasm (Plate 5). Most of the acini had lumina, while some had none. The ducts were lined by simple cuboidal epithelium and were surrounded

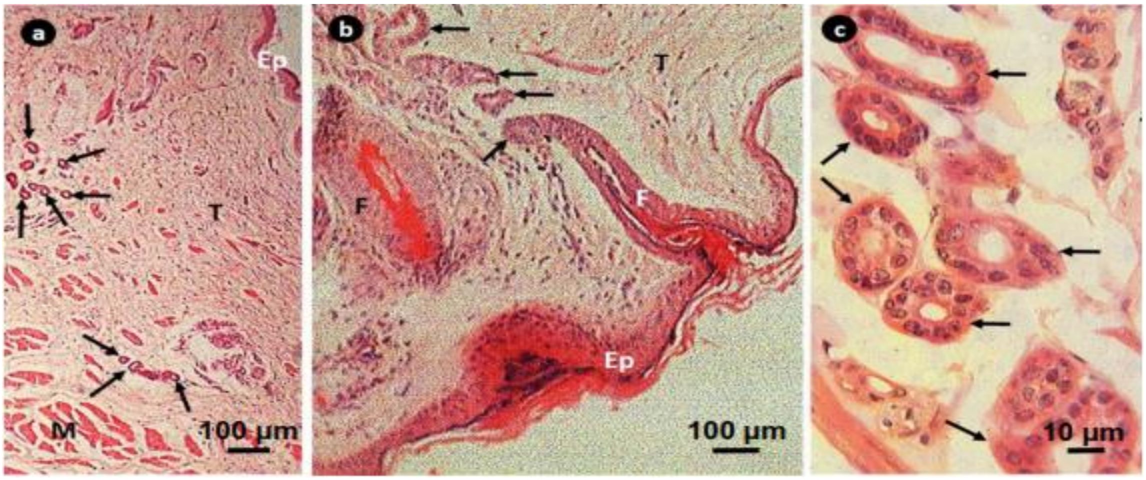

Plate 4: The gland of Moll of the African grasscutter
a. and **b.** Low power micrograph of the eyelid of the African grasscutter showing the epidermis (Ep), tarsal plate (T), skeletal muscle tissue (M), and the simple coiled tubular glands of Moll (arrows), which are associated with hair follicles (F). Haematoxylin and eosin stain. **c.** High power micrograph of the gland of Moll (arrows) showing its simple cuboidal epithelial lining and lumen. Haematoxylin and eosin stain

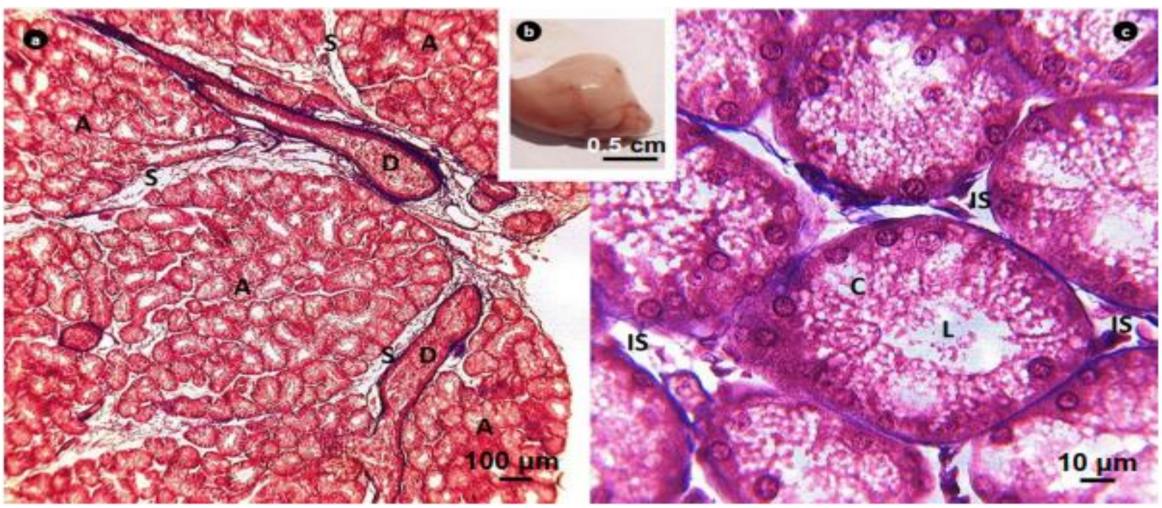

Plate 5: The harderian gland of the African grasscutter
a. Microscopic view of the harderian gland showing the ducts (D) and connective tissue septa (S) which divides the gland into lobules (A). Bluish colouration indicates presence of collagen in the periductal areas. Masson's trichrome stain. **b.** Inset shows gross triangular outline of the gland. **c.** Higher magnification of the gland showing the luminal space (L) and mononuclear columnar cells of the secretory acinus with foamy cytoplasm and basally-located round nuclei. Bluish collagen fibers are seen in the interstitial spaces (IS). Masson's trichrome stain

by numerous collagen fibres.

The suprapalpebral protuberance was noted to increase in size with age in the animals. Histologically, it was a glandular mass divided into lobules by loose connective tissue (Plate 6). Each lobule contained numerous compact secretory acini comprising wedge-shaped mononuclear secretory epithelial cells without a central lumen. These secretory cells exhibited basally-displaced round to oval nuclei and pale-staining foamy cytoplasm. In addition, flat myoepithelial-like cells were sometimes observed at the periphery of the acini. The ducts were lined by simple cuboidal epithelium.

Discussion

The morphology of the rodent skull described in this study is similar to that of other rodents, such as the large South American rodent, capybara (*Hydrochoerus hydrochaeris*) (Hirota *et al.*, 2018). The capybara, however, has a larger and heavier skull with

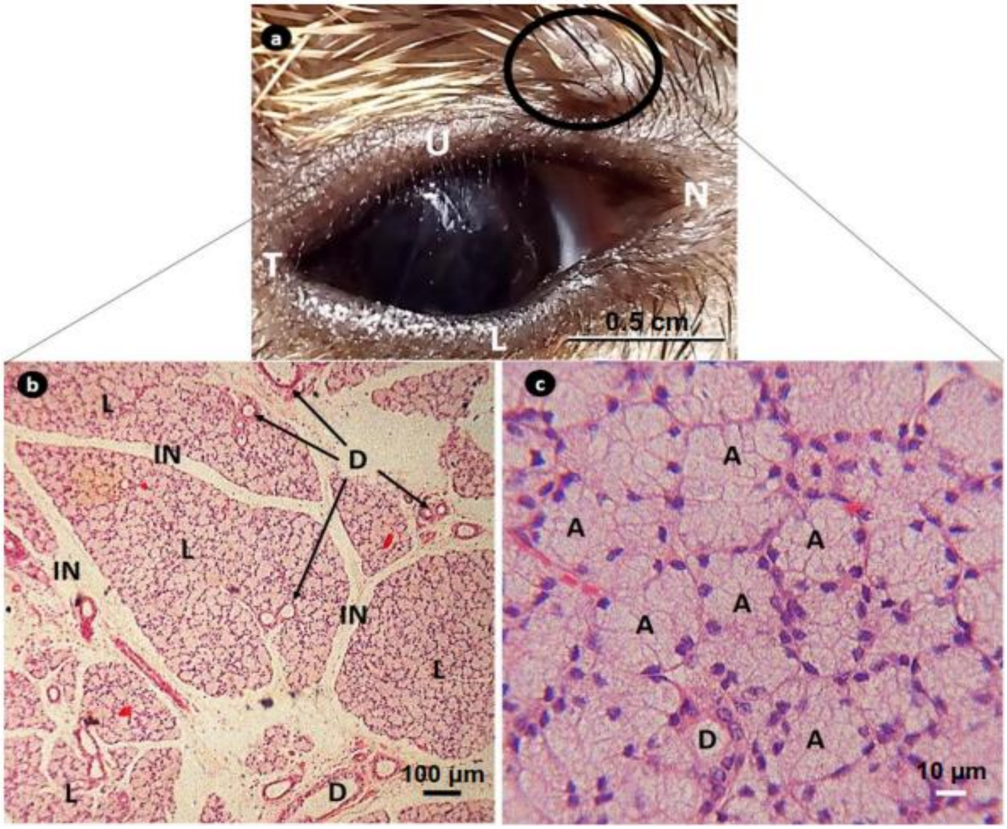

Plate 6: The suprapalpebral protuberance of the African grasscutter
a. Gross appearance of the suprapalpebral protuberance (encircled in black) with the nasal canthus (N), temporal canthus (T), upper eyelid (U), and lower eyelid (L). **b**. Microscopic appearance of the gland showing the numerous lobules (L) and ducts (D) separated by connective tissue septa (IN). Haematoxylin and eosin stain. **c.** Higher magnification of a lobule showing an intralobular duct (D) and numerous compact secretory acini (A) lacking luminal spaces. Haematoxylin and eosin stain

a well-developed lacrimal bone. Laterally situated orbits with their associated higher orbital axis angles as reported in the grasscutter in this study. This is a feature common to rodents. Such monocular orbital configuration is commonly seen in prey animals such as herbivores and permits vision which is especially useful in the wild for easy detection of predators. This could explain why ungulates have been reported to have orbital axis angles of 100^o and above (Shigehara, 1996) with the exception of the tallest terrestrial animal, the giraffe, *Giraffa camelopardalis*, which has been reported to have an orbital axis angle of 60.3 ^{o} (Mitchell *et al.*, 2013). Predator animals such as carnivores and primates, on the other hand, possess more medially situated orbits that permit binocular and stereoscopic vision necessary for an accurate discernment of prey for easy capture. Their orbital axis angles are usually smaller and have been reported to lie between 40 ^{o} and 100 ^{o} (Shigehara, 1996).

The greatly enlarged infraorbital foramen observed in the grasscutter is a morphological trait known as hystricomorphy seen in some clades of rodents (Wood, 1975). Such enlarged foramen have not been reported to possess any visual significance but have been associated with improved chewing efficiency due to the passage of the masseter muscle through it (Swanson *et al*., 2019).

The harderian gland was observed in this study to be the largest ocular gland and was noted to be slightly larger than the eye. Such enormous size could mean that the secretions of the gland are required in copious amounts and/or the gland performs numerous other extra-visual functions. The functions of the gland have been described to not only be the protection and lubrication of the cornea but also as a source of pheromones and thermoregulatory lipids, as well as a site of immune response (Djeridane, 1994). These functions might provide an explanation as to why the gland is further protected by an enveloping layer of simple squamous epithelium instead of a connective tissue layer as seen in other glands. The basally-displaced nuclei and foamy cytoplasm of the cells of its secretory acini, which are histological features associated with mucous cells (Mescher, 2010), suggest the secretions of the gland may be predominantly mucoid. The histological features also indicate that the secretions are produced and stored in the apical portion of the cytoplasm and are released when required by the merocrine method of elaboration. The harderian gland has been reported to occur in most terrestrial vertebrates with nictitating membrane and has been said to contribute lipid secretions to the tear film in rodents (Djeridane, 1994; Payne, 1994) and lagomorphs (Payne, 1994) as well as mucus or serous secretions in the fossorial armadillo and the opossum (Payne, 1994).

The gland of the suprapalpebral protuberance, which we named the suprapalpebral gland in this study, seems not to have been previously described in any rodent species to the best of the knowledge of the authors. The gland shared similar histological features with the harderian gland and can therefore be said to produce mucous secretions. These mucous secretions are known essential components of the tear film of the eye. Their mucin and water components give them their lubricative ability, while their dissolved antiseptic enzymes and normal flora enable them to neutralize and inhibit harmful microbes (Tabak, 1990; Kaplan, 2017). Their thickness and viscosity also form an efficient physical barrier against injurious particulate matter.

The sebaceous glands of Zeis and meibomian glands showed histological features associated with holocrine lipid-secreting glands. Their secretory products may be said to be evenly distributed and stored throughout the cytoplasm, hence the central location of their nuclei. The close association of the glands of Zeis with the palpebral cilia suggests their secretions may be involved solely in the maintenance of the structural integrity of the cilia. This might explain why Zeis gland pathology has been associated with loss of palpebral cilia (Kato *et al*., 1997). The meibomian glands being the most numerous of the palpebral glands, may therefore be solely responsible for the contribution of lipid secretions to the tear film in the grasscutter. The keratinized epithelial lining of its ducts suggests the glandular secretions may be corrosive, a feature that may be helpful in eliminating invading microbes. The Zeis glands and meibomian glands have nevertheless been described as the contributors of the lipid layer of the tear film in humans and animals (Jester *et al.*, 1981; Stoeckelhuber *et al.*, 2003; Knop *et al.*, 2011).

The glands of Moll, being the scantiest and smallest of the glands described in this study, may produce secretions required in small amounts. They can be easily unnoticed in histological sections and may play a role in maintaining the structural and functional integrity of the cilia and palpebral skin. In humans, the gland has been reported to be an apocrine gland with defensive functions (Stoeckelhuber *et al*., 2003; Takahashi *et al*., 2013), while in domestic animals, its functions are said to be unknown (Stoeckelhuber *et al*., 2003; Monteiro-Riviere, 2006).

The lacrimal gland being a major mammalian ocular gland was not described for the grasscutter in this study as it could not be located. Since the gland is reported to be ubiquitous in rodents (Gancharova & Manskikh, 2014), the authors thus believe it is still present in the species and should be an interesting gland to be sought after and investigated in the near future.

In conclusion, this study has shown that the orbital configuration of the grasscutter imparts it with a panoramic field of vision and a hystricomorphous improved masticatory ability while its peri-ocular glands including the tarsal gland, gland of Zeis, gland of Moll, harderian gland, and suprapalpebral gland produce various secretions required for maintenance of the structural and functional integrity of the cornea and eyelid. These secretions are mainly mucoid and lipid. The qualitative and quantitative data from this study will be useful in the identification of orbital and peri-ocular glandular pathology in this species.

Acknowledgements

The authors appreciate the contributions of Dr. Anietie F. Udoumoh who assisted in the revision of the manuscript but declined authorship. We also appreciate the assistance of other staff of the Department of Veterinary Anatomy, Faculty of Veterinary Medicine, University of Nigeria.

Conflict of interest

There is none to be declared

References

Acer N, Sahin B, Ergur H, Basaloglu H & Ceri NG (2009). Stereological estimation of the orbital volume: A criterion standard study. *The Journal of Craniofacial Surgery*, **20**(3): 921–925.

Djeridane, Y (1994). The harderian gland and its excretory duct in the Wistar rat. A histological and ultrastructural study. *Journal of Anatomy*, **184**(3): 553–566.

Gancharova OS & Manskikh VN (2014). Age-related changes in the rat lacrimal gland: Impressive morphology and enigmatic nature. *Russian Journal of Developmental Biology*, **45**(5): 235–242.

Hirota IN, Alves LS, Gandolfi MG, Félix M, Ranzani JJT & Brandão CVS (2018). Tomographic and anatomical study of the orbit and nasolacrimal duct in capybaras (*Hydrochoerus hydrochaeris* — Linnaeus, 1766). *Anatomia Histologia Embryologia*, **47**(4): 298–305.

Igado OO, Adebayo AO, Oriji CC & Oke BO (2016). Cranio-facial and ocular morphometrics of the male greater cane rat (*Thryonomys swinderianus*). *Nigerian Veterinary Journal*, **37**(1): 54–63.

Igbokwe CO, Agina OA, Nwabuisi C & Onoja RI (2017). Haematological and serum biochemistry profile of the juvenile wild African giant rat (*Cricetomys gambianus*, Waterhouse – 1840) in Nsukka, South-Eastern Nigeria – a preliminary investigation. *Journal of Applied Animal Research*, **45**(1): 190–194.

Jester JV, Nicolaides N & Smith RE (1981). Meibomian gland studies: histologic and ultrastructural investigations. *Investigative Ophthalmology & Visual Science*, **20**(4): 537–547.

Kaplan S (2017). *Dear Science: What's the point of mucus?* https://www.washingtonpost.com/news/speaking-of-science/wp/2017/01/09/dear-science-whats-the-point-of-mucus/, retrieved 31-03-2020.

Kato N, Sotodate A & Tomita Y (1997). Zeis Gland Carcinoma. *The Journal of Dermatology*, doi.10.1111/j.1346-8138.1997.tb02299.x.

Knop E, Knop N, Millar T, Obata H & Sullivan, DA (2011). The international workshop on meibomian gland dysfunction: Report of the subcommittee on anatomy, physiology, and pathophysiology of the Meibomian gland. *Investigative Ophthalmology and Visual Science*, **52**(4): 1938–1978.

Lau JCM & Linsenmeier RA (2012). Oxygen consumption and distribution in the Long-Evans rat retina. *Experimental Eye Research*, doi.10.1016/j.exer.2012.07.004.

Mescher AL (2010). Junqueira's Basic Histology, twelfth edition. McGraw-Hill. Pp 84-93.

Miller PE (2008). Orbit. In: *Slatter's Fundamentals of Veterinary Ophthalmology,* fourth edition. (DJ Maggs, PE Miller & R Ofri, editors). Saunders Elsevier. Pp 352–373.

Mitchell G, Roberts DG, van Sittert SJ & Skinner JD (2013). Orbit orientation and eye morphometrics in giraffes (Giraffa camelopardalis). *African Zoology*, **48**(2): 333–339.

Monteiro-Riviere NA (2006). Integument. In: *Dellmann's Textbook of Veterinary Histology,* sixth edition. (JA Eurell & BL Frappier, editors). Blackwell Publishing Limited. Pp. 320–349.

Obadiah B, Dzenda T & Happiness OI (2015). Tail Allometry of the grasscutter (*Thryonomys swinderianus*) and African giant pouched rat (*Cricetomys gambianus*): It's functional relevance. *World Journal of Zoology*, **10**(2): 112–117.

Payne AP (1994). The harderian gland: a tercentennial review. *Journal of Anatomy*, **185**(1): 1–49.

Peter-Ajuzıe IK, Nwaogu IC & Igwebuike UM (2019). Anatomical assessment of the eye of the African grasscutter (Thryonomys swinderianus). *Journal of Applied Life Sciences International*, **20**(2): 1–8.

Sallam HM, Seiffert ER & Simons EL (2011). Craniodental morphology and systematics of a new family of hystricognathous rodents (Gaudeamuridae) from the late eocene and early oligocene of Egypt. *Plos One*, doi.10.1371/journal.pone.0016525.

Samuelson DA (2014). Ophthalmic Structures. In: *Essentials of Veterinary Ophthalmology,* Third edition. (KN Gelatt, editor). John Wiley & Sons Inc. Pp. 12–39).

Shigehara N (1996). Metrical study of the direction of the orbits in primates. *Primate Research*, **12**(2): 165–178.

Stoeckelhuber M, Stoeckelhuber BM & Welsch U (2003). Human glands of moll: Histochemical and ultrastructural characterization of the glands of moll in the human eyelid. *The Journal of Investigative Dermatology*, **121**(1): 28–36.

Sullivan LM & Romney CP (1999). *Cleaning and Preserving Animal Skulls.* www.ag.arizona.edu/pubs/natresources/az1144.pdf, retrieved 17-03-2016.

Swanson MT, Oliveros CH & Esselstyn JA (2019). A phylogenomic rodent tree reveals the repeated evolution of masseter architectures. *Proceedings of the Royal*

Society B, doi.10.1098/rspb.2019.0672.

Takahashi Y, Watanabe A, Matsuda H, Nakamura Y, Nakano T, Asamoto K, Ikeda H & Kakizaki (2013). Anatomy of secretory glands in the eyelid and conjunctiva: A photographic review. *Ophthalmic Plastic and Reconstructive Surgery*, **29**(3): 215–219.

Tabak LA (1990). Structure and function of human salivary mucins. *Critical Reviews in Oral Biology and Medicine*, **1**(4): 229–234.

Wood AE (1975). The Problem of the Hystricognathous Rodents. *Papers on Palaentology*, **3**(12): 75–80.